JTTEE5 14:453-461
DOI: 10.1361/105996305X76450
1059-9630/$19.00 © ASM International

Study on Porosity of Plasma-Sprayed Coatings by Digital Image Analysis Method

Hao Du, Jae Heyg Shin, and Soo Wohn Lee

(Submitted September 20, 2004; in revised form January 5, 2005)

The porosities of plasma-sprayed Al_2O_3, ZrO_2, and TiO_2 coatings deposited on 304 stainless steel plates were evaluated by the digital image analysis method. As the accuracy of this method depends significantly on metallographic preparation and metallography procedure for coating specimens, the effects of cross-surface roughness, magnification, and number of fields of view on the porosity were studied. The results indicate that the porosity value from polished specimen with cross-surface roughness no more than 0.1 μm is acceptable. The porosity value obtained at higher magnification is a little bit higher, especially when the real porosity is higher; more fields of view have to be considered in this case. Both experimental results and statistic analysis suggest that 15 fields of view at 1000× magnification can be implemented to evaluate porosity of plasma-sprayed coating considering both the domain size and the resolution at the same time.

Keywords digital image analysis method, field of view, magnification, plasma-sprayed coating, roughness

1. Introduction

Pores (or voids) are a common feature in plasma-sprayed coatings (Ref 1-4). Their quantity and morphology are very crucial to mechanical and physical properties of the coatings (Ref 5-10). Indeed, the principle behind plasma spray is to melt material feedstock and to accelerate the molten particles until impact on a substrate where rapid solidification and deposit buildup occur. Generally, it has been assumed that porosity has three origins in plasma-sprayed coating. These are interlamellar pores and globular or irregular pores caused by imperfect contact and partially molten particles or gas entrapment (Ref 11), as well as intrasplat cracks due to stress relaxation (Ref 6-8, 12). Other defects, such as splat boundaries, which are difficult to resolve from micrographs since their thickness is near zero (Ref 11), are not always modeled.

Currently, there are numerous methods for porosity measurement for plasma-sprayed coatings, such as digital image analysis (Ref 13-16), mercury intrusion porosimetry (MIP) (Ref 16-19), Brunauer-Emmett-Teller (BET) gas absorption (Ref 18, 20), Archimedean displacement (Ref 11, 21, 22), and small-angle neutron scattering (SANS) (Ref 16). The digital image analysis method quantifies porosity (i.e., average volume fraction of porosity) by image analysis on cross-section views of pore average surface fraction. The accuracy of this method depends significantly on metallographic preparation and metallography procedure for coating specimens. The MIP and BET methods measure porosity gravimetrically by filling the material with a gas or liquid and obtaining the volume of the pores from the mass of the absorbed fluid. However, this procedure requires assuming a constant absorbate density throughout the pore system. In microporous and ultramicroporous materials, where the ratio of surface area to volume is very high, the influence of the pore walls on the packing of gas or liquid molecules may not be negligible and leads to systematic errors in these determinations. Furthermore, the two methods fail to measure open pores accurately. Archimedean displacement porosimetry measures porosity by weighing the mass variation. This method is restricted by the accuracy to weigh the mass loss and the difficulty to estimate the matrix density when allotropic transformation occurs. The SANS method can be used to characterize porosity by the information about the specific void surface area of ceramic deposits. However, the examination of the relationship between the specific void surface area and mechanical properties of deposit yielded a very poor dependence. Furthermore, the volumetrically averaged information in the SANS-based model limited its similarity with the real microstructure. Among all methods, digital image analysis method is more broadly accepted considering reproducibility, economy, simplicity, and versatility for analysis and characterization of coating porosity.

In this work, a digital image analysis method is implemented to evaluate porosities of plasma-sprayed Al_2O_3, ZrO_2, and TiO_2 coatings. The effects of three key factors (i.e., roughness of polished cross surface, magnification, and number of fields of view) on porosity level of these three coatings are studied. Furthermore, reasons for porosity level mismatch are analyzed. Finally, proper values for the three parameters on the basis of both experimental results and statistical analysis are suggested.

2. Experimental Procedures

Three commercial powders, Al_2O_3, ZrO_2, and TiO_2, were used to deposit coating specimens. Both Al_2O_3 and TiO_2 pow-

The original version of this paper was published as part of the DVS Proceedings: "Thermal Spray Solutions: Advances in Technology and Applications," International Thermal Spray Conference, Osaka, Japan, 10-12 May 2004, CD-Rom, DVS-Verlag GmbH, Düsseldorf, Germany.

Hao Du and **Soo Wohn Lee,** Interface Engineering Laboratory, Division of Materials and Chemical Engineering, Sun Moon University, Korea (Dr. Hao Du is now working in Institute of Metal Research, Chinese Academy of Sciences, Shenyang 110016, People's Republic of China); and **Jae Heyg Shin,** Agency for Technology and Standard, Korea. Contact e-mail: hdu72@hotmail.com.

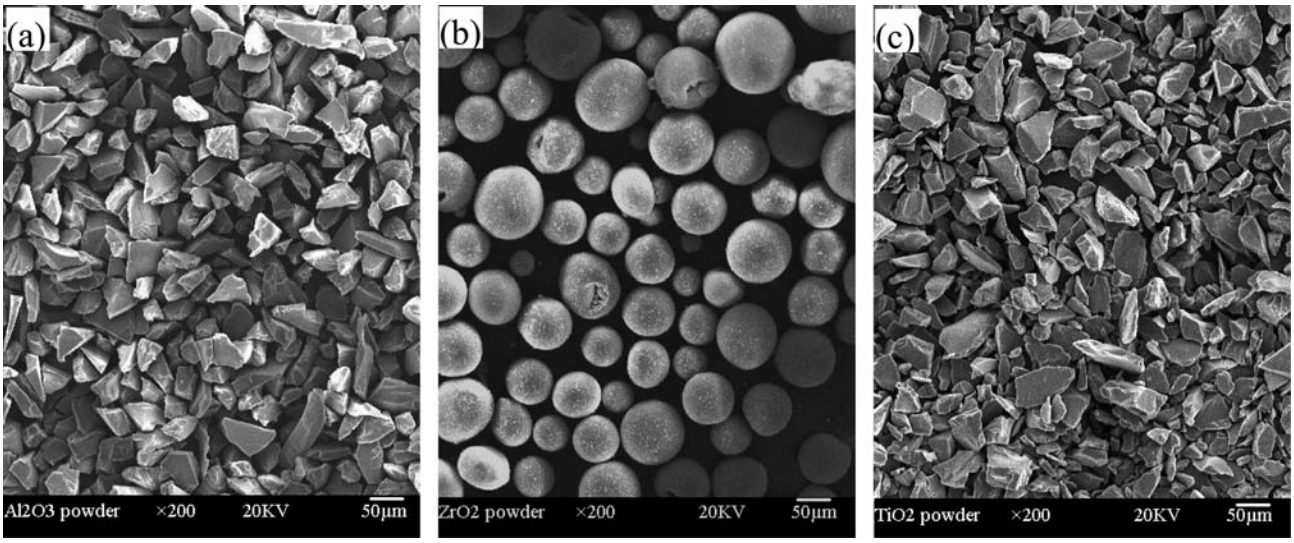

Fig. 1 SEM micrographs of starting powders: (a) Al_2O_3 powder, (b) ZrO_2 powder, and (c) TiO_2 powder

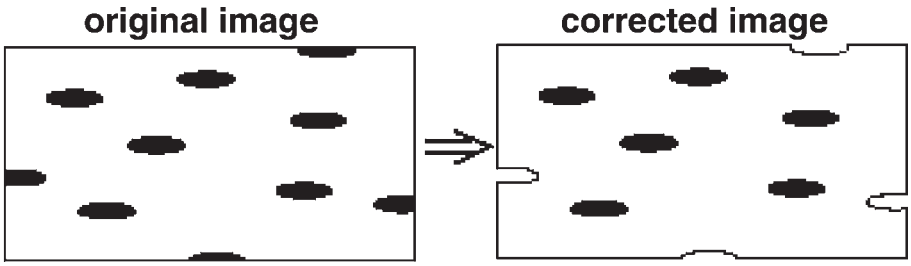

Fig. 2 Sketch map on correction of micrographs prior to carrying out analyses

ders with grain sizes of about 20-50 μm were irregular and angular, while ZrO_2 powders with grain sizes of about 20-70 μm were spherical and near-spherical (Fig. 1).

A Metco A-2000 atmospheric plasma spraying equipment with F4-MB plasma gun (Sulzer Metco AG, Switzerland) was used to deposit the Al_2O_3, ZrO_2, and TiO_2 coatings with parameters listed in Table 1. The plasma jet was fed with a Twin-System 10-C (Plasma-Technik AG, Switzerland). The thickness of as-sprayed coatings was about 400-600 μm. The 304 stainless steel substrates (50 × 20 × 2 mm) were degreased ultrasonically in acetone and grit-blasted with alumina abrasive before spraying.

The morphologies of the starting powders and coatings were observed with a scanning electron microscopy (SEM; JSM 6400, JEOL, Tokyo, Japan). The metallographic process on these coatings is composed of standard sectioning, cleaning, mounting, grinding, and polishing. The cross surface roughness of coating controlled by duration for fine grinding and polishing was measured as Ra (average surface roughness) with Form Talysurf Plus (Rank Taylor Hobson Ltd., Leicester, UK). Three magnifications, 500, 1000, and 2000, with several groups of field of view from 5 to 40 were chosen to quantify porosities of these coatings. For each magnification, the dimension of the field of view and the resolution were 256 × 200 μm, 0.6 μm (500×); 128 × 100 μm, 0.3 μm (1000×); and 64 × 50 μm, 0.15 μm. All fields of view in each group were chosen arbitrarily in sequence, covering the whole sample. The porosity determination

Table 1 Summary of plasma spraying parameters for Al_2O_3, ZrO_2, and TiO_2 coatings

Coating	Al_2O_3	ZrO_2	TiO_2
Current, A	500	620	600
Voltage, V	73	71	67
Ar gas flow, slpm	41	35	40
H_2 gas flow, slpm	14	12	14
Carrier gas flow, slpm	3.5	3.5	3.5
Torch traverse speed mm/s	9.6	9.7	9.6
Spraying distance, mm	130	120	100

on these micrographs works based on the principle of gray value analysis. It should be noted that micrographs were corrected prior to carrying out analysis, features touching the image edges were discarded during the analysis (Fig. 2).

3. Results and Discussion

3.1 Effect of Cross Surface Roughness

Metallographic preparation of plasma-sprayed coating specimens are very important for their porosities. It has always been an issue of discussion and debate. This process and its difficulty depend on the kind of material used and goal. Researchers always judge the preparation using SEM micrographs to confirm that no coarse features occur during the process, which

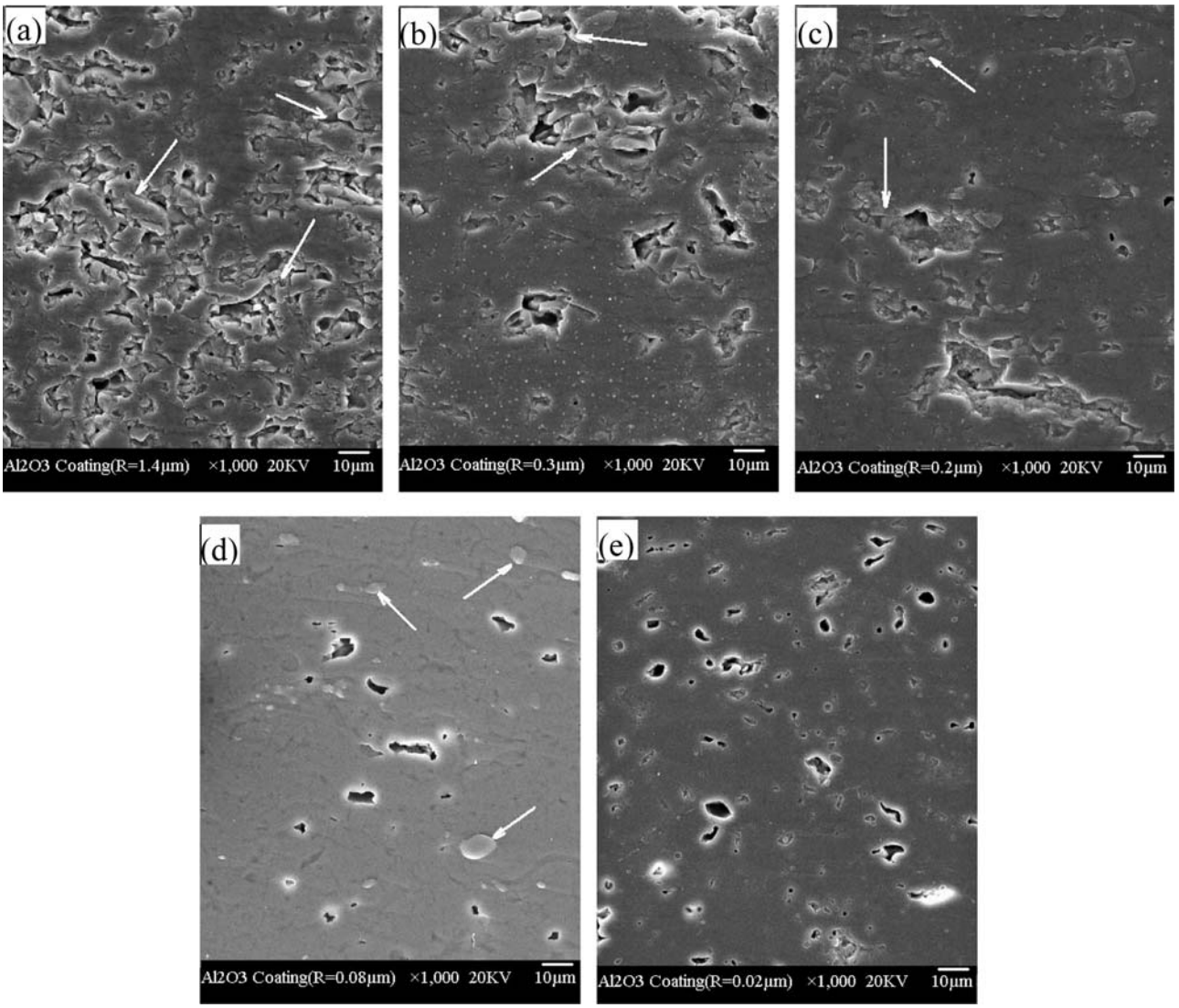

Fig. 3 Cross-surface morphologies of plasma-sprayed Al_2O_3coating with different roughness: (a) 1.4 μm, (b) 0.3 μm, (c) 0.2 μm, (d) 0.08 μm, and (e) 0.02 μm

signifies the presence of pullouts and result inevitably in deviation. As a crucial parameter to evaluate the quantity of the preparation, the effect of surface roughness on porosity level of the three coatings is studied. The roughness ranges from 0.02 to 1.4 μm for the Al_2O_3 coating, 0.02 to 0.6 μm for the ZrO_2 coating, and 0.02 to 0.08 μm for the TiO_2 coating. Twenty fields of view at magnification of 1000 are used for porosity quantification on each coating. The reason for this choice can be found in the following section in detail.

The polished cross-surface micrographs of the three coatings with different roughness at magnification of 1000 are shown in Fig. 3-5. It is apparent that the size and area of pores cannot be distinguished clearly when surface roughness is above 0.2 μm, even when image contrast is modulated. Some areas will be misunderstood and miscalculated as pores, which are pointed by arrows, while such a problem does not appear when the roughness is lower than 0.1 μm. It is reasonable to believe that porosity resulting from specimens with higher roughness is incredible and higher than the real one. It should be noted that the pullouts kept on the cross surface after polishing may occur even the roughness is low, which is shown in Fig. 3(d), this problem will result in the deviation of the porosity result and must be avoided.

Figure 6 shows the effect of surface roughness on the porosity level for the three coatings. The larger the surface roughness is, the higher the porosity. The porosity of the Al_2O_3 coating is 18% when the roughness is 1.4 μm and 15% when the roughness is 0.02 μm; about 20% deviation occurs between the two results. The same change appears on the ZrO_2 coating. It is worth pointing out that no more than 5% deviation on porosity occur when cross surface roughness of coating decreases from 0.1 to 0.02 μm.

It is accepted that the porosity resulting from the coating cross surface with lower roughness is more accurate. However, it should be noted that the roughness depends on not only preparation process but also porosity, as well as pore size and distribution of the coating. On the other hand, a new problem on specimen preparation for lower surface roughness appears, both more care and longer time must be spent on it. Furthermore, it is

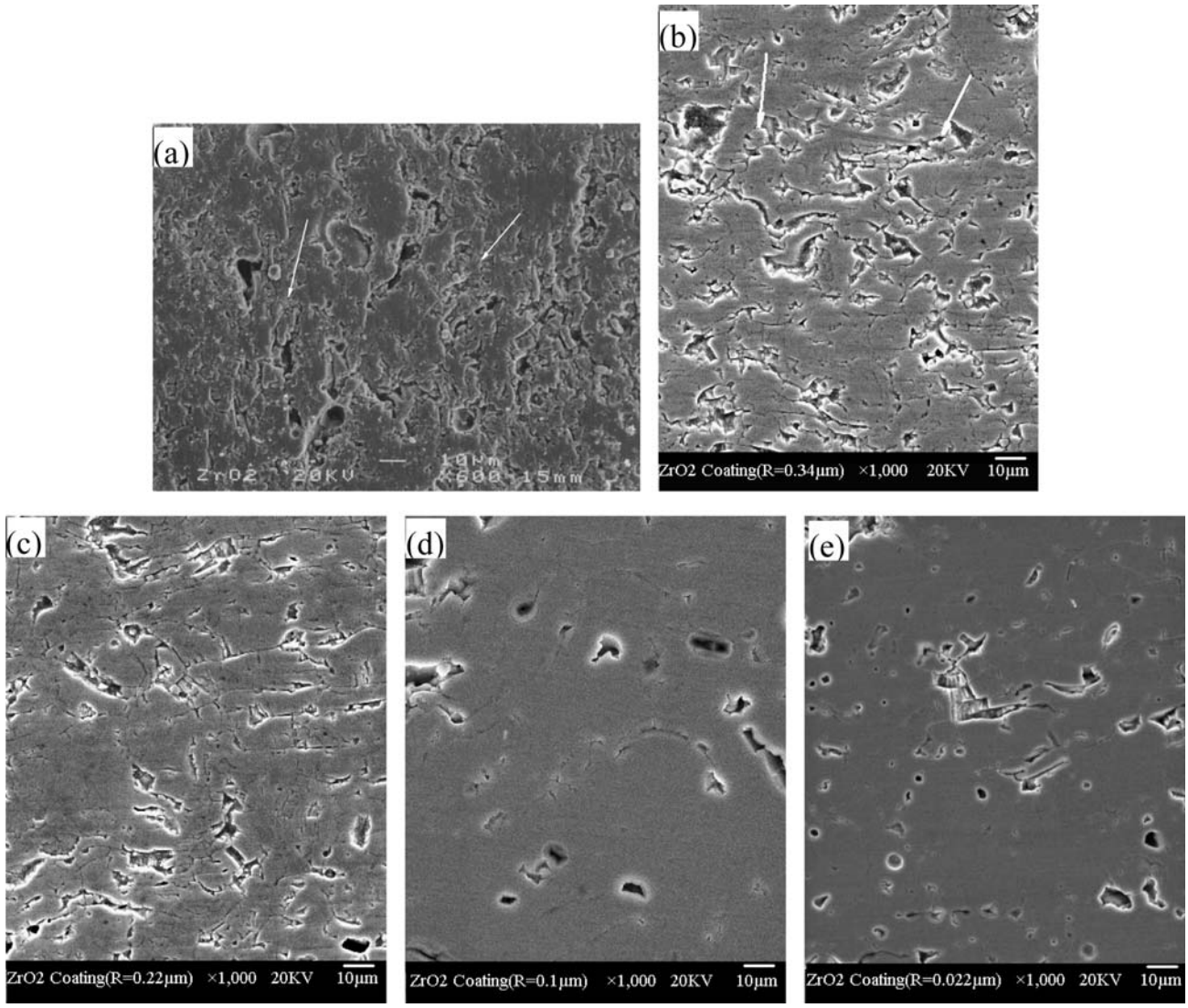

Fig. 4 Cross-surface morphologies of plasma-sprayed ZrO_2 coating with different roughness: (a) 0.6 μm, (b) 0.34 μm, (c) 0.22 μm, (d) 0.1 μm, and (e) 0.022 μm

very hard, even impossible to prepare some kind of coating specimens with very low roughness. In this study, accuracy cannot be improved remarkably when coating cross-surface roughness is changed from 0.1 to 0.02 μm on both Al_2O_3, and ZrO_2 coatings with higher porosity (15%, 14.3%) and the TiO_2 coating with lower porosity (2.8%). Therefore, in view of both accuracy and difficulty on sample preparation, 0.1 μm is suggested as the largest surface roughness for porosity measurement of plasma-sprayed Al_2O_3, ZrO_2, and TiO_2 coatings by the digital image analysis method. There may be a little adjustment on this value for other kinds of coatings on the basis of their special conditions.

3.2 Effects of Magnification and Number of Fields of View

It has been mentioned that porosity measurement by the digital image analysis method considers a small domain to represent a coating. Generally, the model specimen must be large enough to contain sufficient microstructural features so that a representative porosity level can be obtained. If the modeling surface is too small, the numerical results may not be average due to the stochastic nature of the plasma-spray microstructure, as well as numerical artifacts introduced at the boundaries. Furthermore, high graphic resolution (controlled by the microscope magnification) is necessary to capture thin cracks; otherwise, they do not appear in the micrograph. These considerations have to be taken into account during the metallographic procedures. Thus, for a given computational resource, the process usually requires a compromise between the domain size and the model resolution. It should be kept in mind that the key element of image analysis approach for porosity is to identify and model the volumetrically averaged microstructural features instead of the realistic microstructural details, such as pore size and distribution. Therefore, deliberately choosing micrograph areas without unusually large pores should be avoided; it is also un-

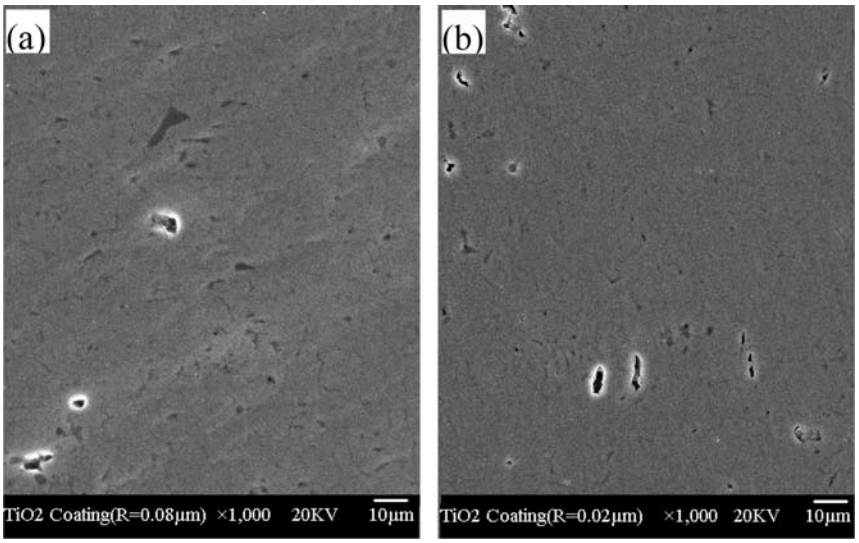

Fig. 5 Cross-surface morphologies of plasma sprayed TiO_2 coating with different roughness: (a) 0.08 μm and (b) 0.02 μm

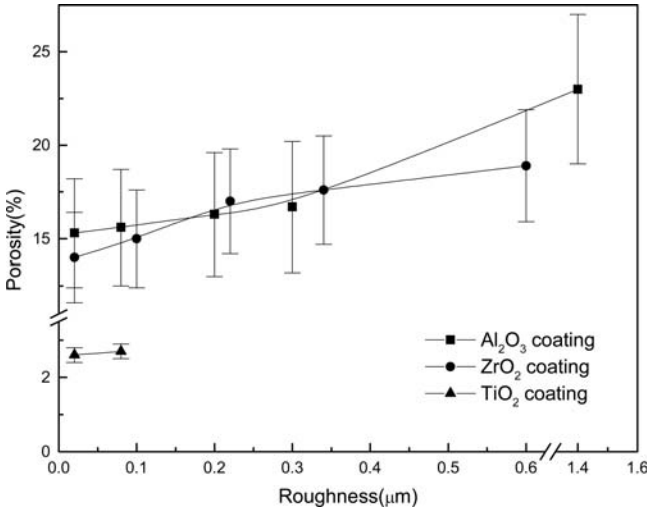

Fig. 6 Effect of surface roughness on porosity for plasma sprayed Al_2O_3, ZrO_2, and TiO_2 coatings

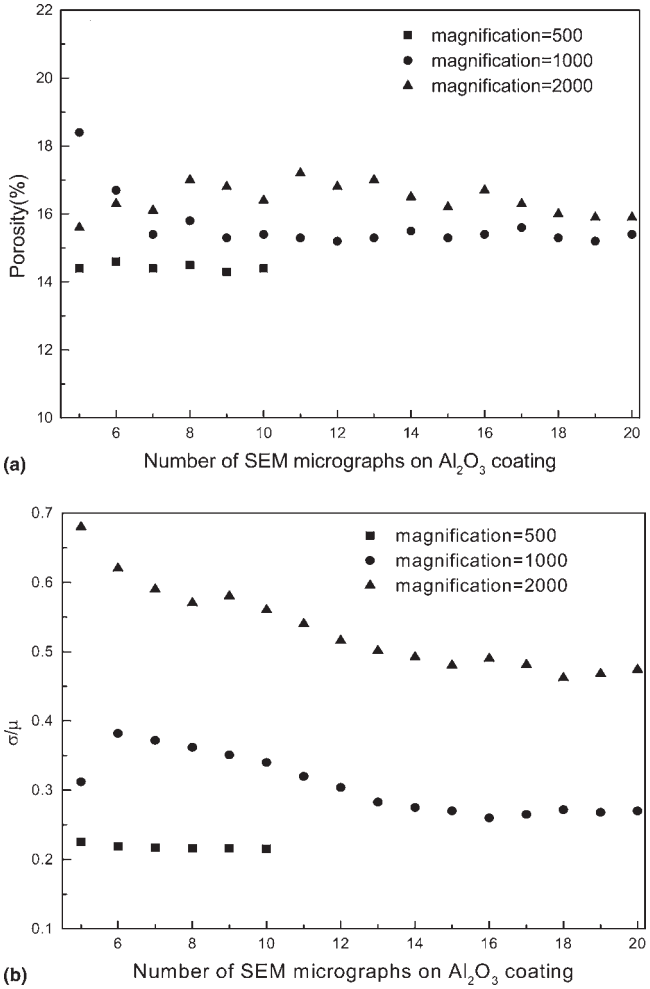

Fig. 7 Effect of magnification and number of fields of view on (a) porosity and (b) measurement variability of plasma sprayed Al_2O_3 coatings

necessary to choose so many areas to represent sufficient microstructural details.

It is contradictory to balance accuracy and field area of view for porosity of plasma-sprayed coating. A compromise should be made where both the sampling problem and accuracy of measurement are satisfied to some extent. Many researchers and engineers reported their results at magnifications of 400, 500, 800, 1000, 1500, and 2000 and with a number of fields of view 10, 15, 20, and 30 (Ref 15, 23-25). In this study, both parameters are considered.

The effects of magnification and the number of fields of view on the porosity level and measurement variability of the three coatings are shown in Fig. 7-9. As the overall porosity came from several local values, which vary from selected micrographs, it apparently changed, especially when no more than 5

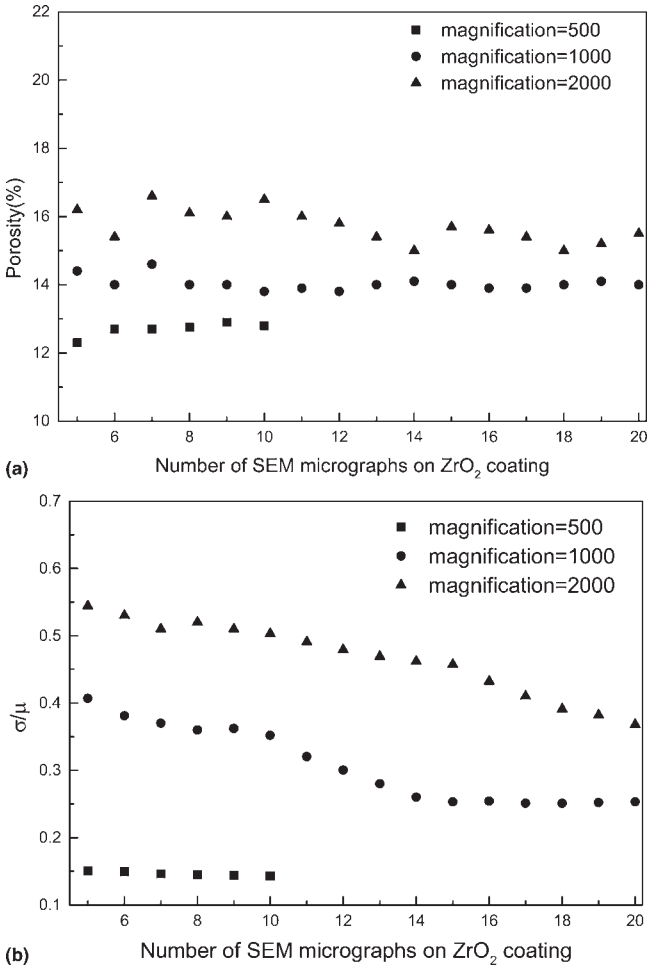

Fig. 8 Effect of magnification and number of fields of view on (a) porosity and (b) measurement variability of plasma sprayed ZrO_2 coatings

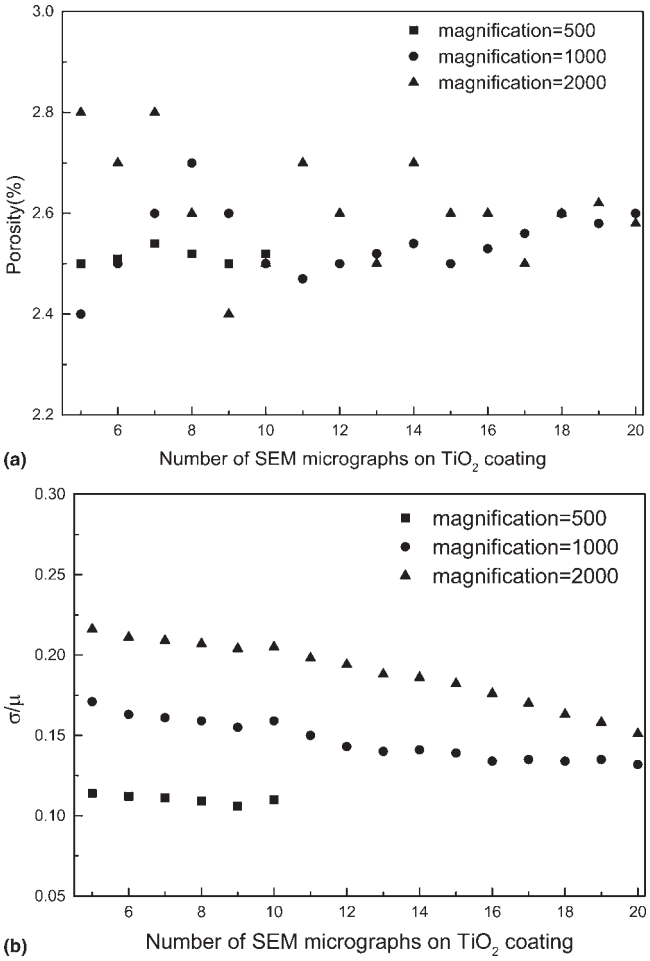

Fig. 9 Effect of magnification and number of fields of view on (a) porosity and (b) measurement variability of plasma-sprayed TiO_2 coatings

micrographs were used. It is clear that the lower the magnification, the more quickly the porosity and the measurement variability reach stabilized values. When magnification of 500 is chosen, stabilized value on porosity and measurement variability can be obtained with 6-7 micrographs for the three coatings. When magnification is 1000, stabilized values can be obtained with 14-15 micrographs for the Al_2O_3, ZrO_2 coatings and with 12-13 micrographs for the TiO_2 coating. In the case of magnification of 2000, stabilized values on porosity and measurement variability can be obtained with 17-19 micrographs for the Al_2O_3 and ZrO_2 coatings and with 20 micrographs for the TiO_2 coating. This distinction can be attributed to the different areas covered in one micrograph at different magnifications. The relationship of the field size of the view at magnifications of 500, 1000, and 2000 is shown in Fig. 10. The field size of view at magnification of 500 is 4 times that at magnification of 1000 and 16 times that at magnification of 2000. If 16 micrographs at magnification of 2000 were taken instead of a micrograph at magnification of 500, the same field size can be kept and the accuracy for porosity will be improved. On the other hand, the same work has to be repeated for 16 times. As porosity is a statistic medium value, many fields of view have to be chosen for it,

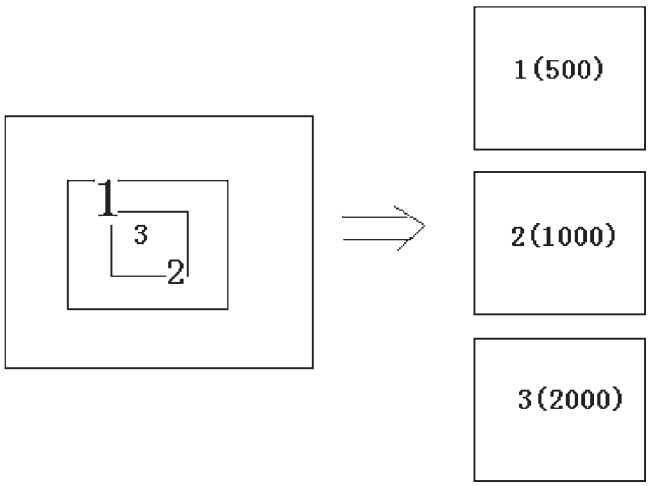

Fig. 10 Sketch map on relationship of fields of view at different magnifications

especially when the coating is not homogeneous. A larger area is covered in one micrograph when magnification is equal to 500, so a stabilized value on porosity can be approached more quickly

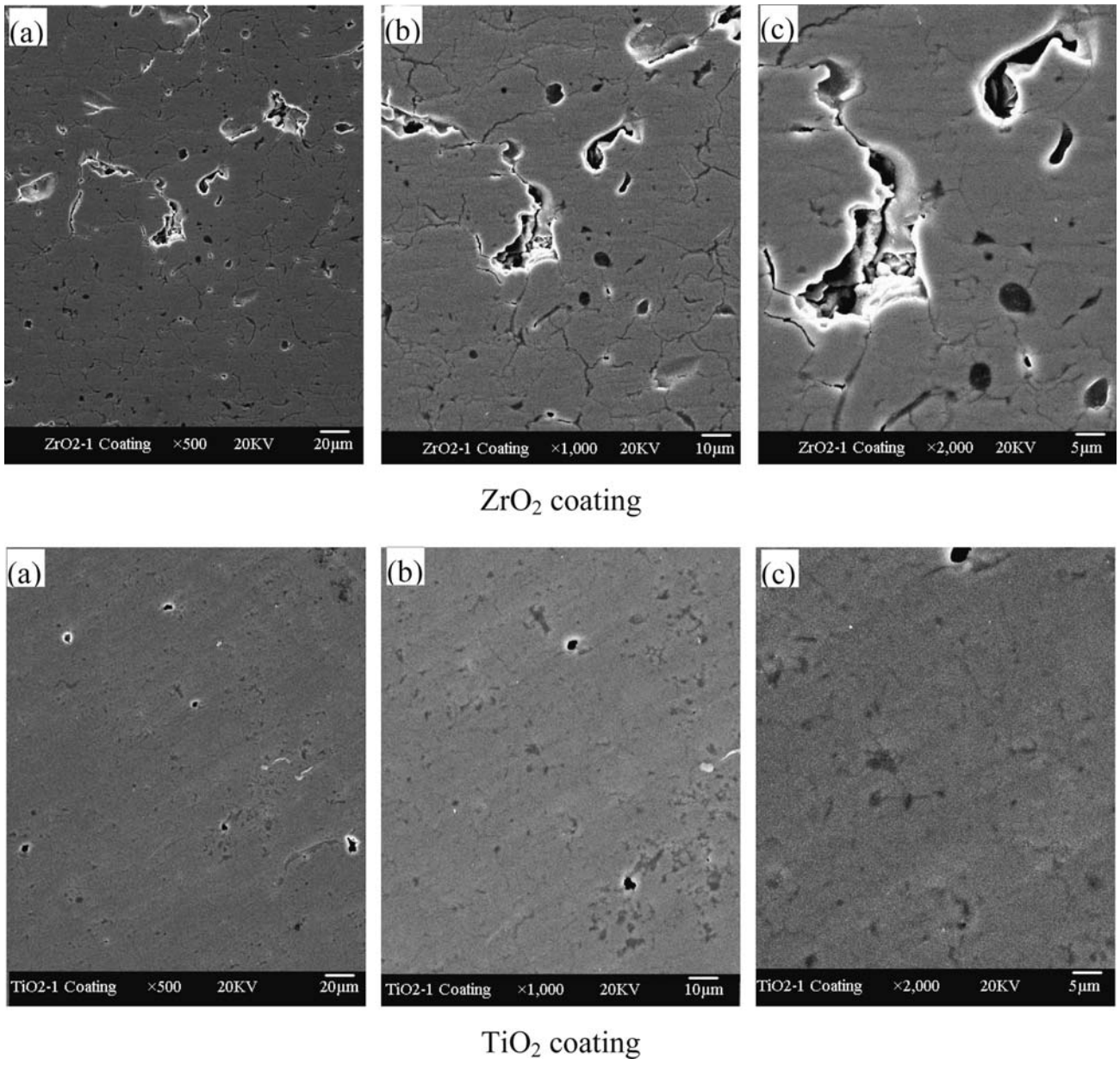

Fig. 11 Comparison of plasma-sprayed ZrO_2 and TiO_2 coatings with the same center field of view but at three different magnifications: (a) 500×, (b) 1000×, and (c) 2000×

at this magnification. Also, it should be noted that porosity results at different magnification approach each other at last. This approach is more obvious on the TiO_2 coating than on the other two coatings due to its lower porosity. It can be predicted that such an approach can be achieved on the Al_2O_3 and ZrO_2 coatings when more fields of view are chosen.

It is interesting to note that higher porosity levels of the Al_2O_3 and ZrO_2 coatings obtained at higher magnification with the same number of fields of view are higher, especially when no more than 10 fields of view are chosen; the opposite occurs for the TiO_2 coating. This can be explained by the larger porosities characterizing Al_2O_3 and ZrO_2 coatings. The possibility of pores caught by fields of view at higher magnification is larger if more pores exist in coating, which leads to porosity higher than the real one when enough field of view on cross surface of coating cannot be guaranteed. If pores, especially the larger ones, are caught in a micrograph when magnification is chosen as 2000, the porosity from it is much higher than the real value. Otherwise, it is much lower. Figure 11 illustrates this assertion on ZrO_2 and TiO_2 coatings with the same center field of view but at three different magnifications. There are some pores in the field of view when the magnification is 500. Those that also appeared in micrographs at magnifications of 1000 and 2000 are enlarged about 4 and 16 times, respectively; the porosity becomes very high, especially for ZrO_2 coating. The porosity level varies from 7% (500×) to 11% (1000×) and 21% (2000×). The opposite re-

Table 2 Porosity of plasma-sprayed Al_2O_3, ZrO_2, and TiO_2 coatings by statistical point

Porosity, %	500 (20)	1000 (15)	1000 (20)	2000 (20)	1000 (40)
Reliability = 0.99					
Al_2O_3 coating	14.6 ± 2.0	15.3 ± 3.4	15.4 ± 2.9	15.9 ± 4.6	15.4 ± 1.9
ZrO_2 coating	12.9 ± 1.1	14.1 ± 3.0	14.0 ± 2.4	15.5 ± 3.9	14.0 ± 1.5
TiO_2 coating	2.5 ± 0.2	2.5 ± 0.3	2.6 ± 0.2	2.6 ± 0.3	2.6 ± 0.2
Reliability = 0.98					
Al_2O_3 coating	14.6 ± 1.8	15.3 ± 3.1	15.4 ± 2.6	15.9 ± 4.1	15.4 ± 1.7
ZrO_2 coating	12.9 ± 1.0	14.1 ± 2.6	14.0 ± 2.2	15.5 ± 3.5	14.0 ± 1.3
TiO_2 coating	2.5 ± 0.1	2.5 ± 0.2	2.6 ± 0.2	2.6 ± 0.2	2.6 ± 0.1

Table 3 Relationship between magnification, number of fields of view, and porosity deviation of the plasma sprayed Al_2O_3, ZrO_2, and TiO_2 coatings (Reliability = 0.98)

S*, %	500	1000	2000
Al_2O_3 coating			
5	3.6	6.5	11.9
10	3.1	5.9	9.7
15	3.0	4.3	8.1
20	3.0	4.3	7.7
ZrO_2 coating			
5	2.0	6.6	9.9
10	1.9	5.1	8.8
15	1.8	3.7	7.4
20	1.7	3.6	5.8
TiO_2 coating			
5	0.3	0.5	0.7
10	0.3	0.4	0.5
15	0.2	0.4	0.5
20	0.2	0.3	0.4

sults will be found if not all pores appear in the micrographs at the magnifications of 1000 or 2000, which can be found on the TiO_2 coating. Its porosity level varies from 3% (500×) to 2.4% (1000×) and 2% (2000×). It is worth pointing out that this deviation in the single micrograph is eliminated if more fields of view can be supplied.

It should be noted that the small interlamellar pores and intrasplat cracks may remain unresolved at lower magnification, and play another role on the deviation of porosity from different magnifications.

3.3 Statistical Analysis

Porosity of a coating is an averaged value; the fields of view have to be chosen randomly for it. To make sure the averaged features of the entire coating can be represented by several small domains, the report of porosity from the statistic view is necessary. The main idea of statistical theory for porosity is deriving collective microstructral information from several small domains.

Table 2 shows a porosity level of the Al_2O_3, ZrO_2, and TiO_2 coatings by statistic points. The reported porosities are composed of average values and deviation ranges. It is clear that the deviation ranges have to be wider when the reliability is higher. At the same time, the deviation range is narrower when more fields of view are chosen, which is shown in comparison between 15, 20, and 40 micrographs at magnification of 1000. On the other hand, the deviation range is wider when the magnification of views increases, which is shown in comparison between 500, 1000, and 2000 with 20 micrographs. These results indicate that at a proper reliability, fewer fields of view can result in a proper range at lower magnification. At a proper magnification, more fields of view can result in a more reliable porosity with narrower range. It should be noted that the improvement is not very important on the average porosity and deviation range when more than 15 micrographs are chosen. When 15, 20, and 40 micrographs at magnification of 1000 are chosen for porosity, the average value changed from 15.3, 15.4, to 15.4% on the Al_2O_3 coating, 14.0, 14.0, to 14.0% on the ZrO_2 coating, and 2.5, 2.6, to 2.6% on the TiO_2 coating, respectively. Their value fluctuations are no more than 0.5%. It can be found that more micrographs are useful only to a narrow deviation range; this means at a special reliability most of individual porosity from new micrographs is also in this range, and they play an important role for the narrow.

Table 3 shows the relationship between magnification, number of field of view, and porosity deviation for the Al_2O_3, ZrO_2, and TiO_2 coatings when the reliability is 98%. Their deviations indicate the fluctuation of porosity at a proper magnification with different number of fields of view. The scatter on average deviation can be found clearly when no more than 5, 15, and 25 micrographs at magnifications of 500, 1000, and 2000 are used. Furthermore, these values remain stabilized when more data points are added. At the same time, fewer data points can result in a stabilized deviation, which appears more quickly for lower magnification and agrees with the experimental results introduced above. It should be noted that the deviation mentioned here is the average difference between each porosity and average porosity of the coating, by which the porosity range can be calculated. By these results on an average deviation of the three coatings, porosity of plasma sprayed coating from more than 15 fields of view is reliable when magnification is chosen as 1000.

4. Conclusions

Digital image analysis method on cross-section views is widely used to evaluate the porosity of plasma-sprayed coating. Parameters, such as cross-surface roughness, magnification of the view, and the number of fields of view in metallographic preparation and metallography procedure are crucial to the evaluation. More accurate results can be obtained with lower cross-surface roughness, more fields of view, and higher magnification of view. The results indicate roughness of polished cross section no more than 0.1 μm should be guaranteed for porosity evaluation of plasma-sprayed coating by this method. Based on both experimental results and statistical analysis, at

least 15 fields of view at magnification of 1000 on cross sections are suggested for the porosity measurement of plasma-sprayed coatings due to balancing accuracy and field area of view; the values mentioned above may be adjusted by pores size and quantity.

Acknowledgment

This work was supported by the program ITEP 1005583 (Korea).

References

1. R.G. Munro, Effective Medium Theory of the Porosity Dependence of Bulk Moduli, *J. Am. Ceram. Soc.,* Vol 84 (No. 5), 2001, p 1190-1192
2. R.W. Rice, Relation of Tensile Strength-Porosity Effects in Ceramics to Porosity Dependence of Young's Modulus and Fracture Energy, Porosity Character and Grain Size, *Mater. Sci. Eng. A,* Vol 112, 1989, p 215-224
3. R.W. Rice, The Porosity Dependence of Physical Properties of Materials: A Summary Review, *Key Eng. Mater.,* Vol 115, 1995, p 1-20
4. R.W. Rice, Evaluation and Extension of Physical Property-Porosity Models Based on Minimum Solid Area, *J. Mater. Sci.,* Vol 31, 1996, p 102-118
5. K.K. Phani and S.K. Niyogi, Elastic Dependence of Ultrasonic Velocity and Elastic Modulus in Sintered Uranium Dioxide, *J. Mater. Sci. Lett.,* Vol 5, 1986, p 427-430
6. A. Nagarajan, Ultrasonic Study of Elasticity-Porosity Relationship in Polycrystalline Alumina, *J. Appl. Phys.,* Vol 42 (No. 10), 1971, p 3693-3696
7. W. Kreher, Ultrasonic Waves in Porous Ceramics with Non-Spherical Holes, *Ultrasonics,* Vol 15 (No. 2), 1977, p 70-74
8. D.N. Bocaacini and A.R. Boccaccini, Dependence of Ultrasonic Velocity on Porosity and Pore Shape in Sintered Materials, *J. Nondestruct. Eval.,* 1997, Vol 16 (No. 4), p 187-192
9. L.C. Erickson, H.M. Hawthorne, and T. Troczynski, Correlations between Microstructural Parameters, Micromechanical Properties, and Wear Resistance of Plasma Sprayed Ceramic Coatings, *Wear,* Vol 250, 2001, p 569-575
10. S.J. Bull, R. Kingswell, and K.T. Scott, The Sliding Wear of Plasma Sprayed Alumina, *Surf. Coat. Technol.,* Vol 82, 1996, p 218-225
11. Z. Wang, A. Kulkarni, S. Deshpanda, T. Nakamura, and H. Herman, Effects of Pores and Interfaces on Effective Properties of Plasma Sprayed Zirconia Coatings, *Acta Mater.,* 51, 2003, p 5319-5334
12. A. Kulkarni, A. Vaidya, A. Goland, S. Sampath, and H. Herman, Processing Effects on Porosity-Property Correlations in Plasma Sprayed Yttria-Stabilized Zirconia Coatings, *Mater. Eng. A,* Vol 359, 2003, p 100-111
13. S.H. Kwon, Y.K. Jun, S.H. Hong, I.S. Lee, and H.E. Kim, Calcium Phosphate Bioceramics with Various Porosities and Dissolution Rates, *J. Am. Ceram. Soc.,* Vol 85 (No. 12), 2002, p 3129-3131
14. Y. Zeng, S.W. Lee, and C. Ding, Study on Plasma Sprayed Boron Carbide Coating, *J. Therm. Spray Technol.,* Vol 11 (No. 1), 2002, p 129-133
15. K.W. Schlichting, N.P. Padture, and P.G. Klemens, Thermal Conductivity of Dense and Porous Yttria-Stabilized Zirconia, *J. Mater. Sci.,* Vol 36, 2001, p 3003-3010
16. C-J. Li and A. Ohmori, Relationships between the Microstructure and Properties of Thermally Sprayed Deposits, *J. Therm. Spray Technol.,* Vol 11 (No. 3), 2002, p 365-374
17. M. Oya and M. Takahashi, Mercury Intrusion Porosimetry, *Am. Ceram. Soc. Bull.,* Vol 81 (No. 3), 2002, p 12-16
18. S. J. Dapkunas, Measurement Methods and Standards for Proccessing and Application of Thermal Barrier Coatings, *J. Therm. Spray Technol.,* Vol 6 (No. 1), 1997, p 67-76
19. K.A. Khor, C.S. Yip, and P. Dheang, Ti-6Al-4V/Hydroxyqpatite Composite Coatings Prepared by Thermal Spray Techniques, *J. Therm. Spray Technol.,* Vol 6 (No. 1), 1997, p 109-115
20. J. Kim, O. Wilhelm, and S.E. Pratsinis, Packaging of Sol-Gel-Made Porous Nanostructured Titania Particles by Spray Drying, *J. Am. Ceram. Soc.,* Vol 84 (No. 12), 2001, p 2802-2808
21. J. F. Yang, T. Ohji, S. Kanzaki, A. Diaz, and S. Hampshire, Microstructure and Mechanical Properties of Silicon Nitride Ceramics with Controlled Porosity, *J. Am. Ceram. Soc.,* Vol 85 (No. 6), 2002, p 1512-1516
22. W.V. Vadakan and G.W. Scherer, Measuring Permeability of Rigid Materials by a Beam-Bending Method: Cement Paste, *J. Am. Ceram. Soc.,* Vol 85 (No. 6), 2002, p 1537-1544
23. R. Dutton, R. Wheeler, K.S. Ravichandran, and K. An, Effect of Heat Treatment on the Thermal Conductivity of Plasma-Sprayed Thermal Barrier Coatings, *J. Therm. Spray Technol.,* Vol 9 (No. 2), 2000, p 204-209
24. M. Prystay, P. Gougeon, and C. Moreau, Structure of Plasma-Sprayed Zirconia Coatings Tailored by Controlling the Temperature and Velocity of the Sprayed Particles, *J. Therm. Spray Technol.,* Vol 10 (No. 1), 2001, p 67-75
25. F. Cernuschi, P. Bianchi, M. Leoni, and P. Scardi, Thermal Diffusicity/Microstructure Relationship in Y-PSZ Thermal Barrier Coatings, *J. Therm. Spray Technol.,* Vol 8 (No. 1),1999, p 102-109